

video-SALMONN S: Memory-Enhanced Streaming Audio-Visual LLM

Guangzhi Sun^{1,2} Yixuan Li¹ Xiaodong Wu² Yudong Yang¹ Wei Li³ Zejun Ma³ Chao Zhang¹

Abstract

Long-duration streaming video understanding is fundamental for future AI agents, yet remains limited by ineffective long-term memory. We introduce video-SALMONN S, a memory-enhanced streaming audio-visual large language model that processes over 3-hour videos at 1 FPS and 360p resolution, outperforming strong non-streaming models under the same memory budget. In addition to token merging or downsampling, video-SALMONN S is the first to employ *test-time training* (TTT) as a streaming memory mechanism for video understanding. TTT continuously transforms short-term multimodal representations into long-term memory embedded in model parameters. To improve long-range dependency modeling and memory capacity, we propose (i) a TTT_{MEM} layer with an additional long-span prediction objective, (ii) a two-stage training scheme, and (iii) a modality-aware memory reader. We further introduce the episodic learning from video memory (ELViM) benchmark, simulating agent-like scenarios where models must learn from videos observed hours earlier. video-SALMONN S consistently outperforms both streaming and non-streaming baselines by 3-7% on long video benchmarks. Notably, video-SALMONN S achieves a 15% absolute accuracy improvement over strong non-streaming models on ELViM, demonstrating strong learning abilities from video memory.¹

1. Introduction

Processing video streams of any length at a fixed high frame rate and a decent resolution is one of the crucial abilities in future AI agents. Despite the rapid progress in state-of-the-art (SOTA) video large language models (LLMs) (Li

¹Tsinghua University ²University of Cambridge ³ByteDance. Correspondence to: Chao Zhang <cz277@tsinghua.edu>.

Preprint. February 4, 2026.

¹<https://github.com/bytedance/SALMONN/tree/video-salmonn-S>

et al., 2024; Zhang et al., 2024c; Wang et al., 2024a; Lin et al., 2024b; Bai et al., 2025b; Zhang et al., 2025a; Tang et al., 2025a; Sun et al., 2025), most of them only perform offline video understanding by setting a maximum number of input visual tokens to the Transformer, hence yielding a significant information loss for long videos. Some recent work explores token compression methods to achieve longer video understanding (Li et al., 2025; Tan et al., 2024; Tang et al., 2025b; Chen et al., 2024; Zhang et al., 2025c), especially ones using the user prompt to achieve high compression ratios (Gao et al., 2024; Wang et al., 2025b).

In real-world scenarios, where both video length and the timing of user queries are typically unknown, offline formulations become challenging to deploy due to the limited attention span of Transformer architectures. This has led to streaming video understanding models that operate at a fixed frame rate and maintain bounded memory via token merging or discarding (Qian et al., 2025; Yang et al., 2025b; Song et al., 2024; Zhang et al., 2025b; Huang et al., 2025; Zeng et al., 2025). While effective for short streams, these methods incur cumulative information loss over long durations, often underperforming relative to offline models. Recent extensions leverage agentic frameworks with external memory (Long et al., 2025) or task-specific frame selection, such as for spatial reasoning (Yang et al., 2025a), but typically require specialized training data or complex memory designs, limiting scalability and practical deployment.

To address these limitations, we propose video-SALMONN S, a streaming audio-visual LLM that achieves SOTA performance on videos exceeding 3 hours in length at 1 FPS and 360p resolution under a fixed memory budget. To the best of our knowledge, video-SALMONN S is the first streaming video LLM to incorporate test-time training (TTT) as a mechanism for enhancing memory. Unlike existing memory consolidation approaches, TTT enables online adaptation through fast-weight updates, allowing model parameters to function as an implicit, parameter-based memory for integrating long-term information. Specifically, we propose the TTT_{MEM} layer, which extends traditional TTT formulations (Sun et al., 2024; Dalal et al., 2025) by incorporating a long-span prediction objective to strengthen long-context modeling. The TTT_{MEM} layer is trained using a two-stage strategy: a cold-start stage that optimizes static TTT parameters with medium-length contexts, followed by a scale-up

stage that progressively expands both context length and memory capacity. At last, we employ a modality-aware, prompt-dependent memory reading mechanism that recurrently compresses multimodal KV caches while strictly adhering to streaming constraints with constant memory usage.

To reflect the practical requirement of long-term memory in video-based agents that operate continuously over streaming inputs, we introduce the **episodic learning from video memory (ELViM)** benchmark. ELViM is the first benchmark explicitly designed to evaluate whether streaming video LLMs can acquire procedural knowledge from past video experiences and reuse it for real-time decision-making. In contrast to existing video benchmarks that focus primarily on short-term perception or within-clip reasoning, ELViM directly assesses the ability to consolidate, retain, and recall information from videos observed hours earlier under realistic streaming constraints. Main contributions are summarised as follows:

- We propose video-SALMONN S, a SOTA streaming audio-visual LLM and the first to leverage TTT as a streaming memory mechanism, enabling over 3 hours of video understanding at 1 FPS and 360p under a fixed memory budget through a novel TTT_{MEM} layer, tailored training loss and scheme and memory-reading designs.
- We propose ELViM, the first benchmark designed to explicitly evaluate whether streaming video LLMs can learn procedural knowledge from past video memory. ELViM provides a principled evaluation for long-term memory and continual learning in streaming video LLMs.
- video-SALMONN S is evaluated on a range of online and general video understanding benchmarks. In particular, video-SALMONN-S consistently exceeds strong streaming and non-streaming baselines by 3-7% in absolute accuracy on long video benchmarks, with 15% accuracy improvement on ELViM.

2. Related Work

2.1. Long Video Understanding

The key challenge of long video understanding is efficient compression of information into a size that the LLM can process. A number of training-based methods (Li et al., 2025; Zhang et al., 2024b; Shen et al., 2024; Shu et al., 2024; Liu et al., 2025a) have been proposed to reduce the number of visual tokens needed to represent each video frame. Some recent visual LLMs, such as Qwen2.5-VL (Bai et al., 2025b), inherently contain token merging modules and a much longer context LLM backbone that are suitable for long video understanding. Meanwhile, training-free methods (Liu et al., 2025b; Zhang et al., 2024d; Yang et al., 2025b; Wang et al., 2024c; 2025b) are also investigated, which mainly select the key-value (KV) cache in

each Transformer block. Specifically, ReTaKe (Wang et al., 2024c) applies a dynamic KV-cache compression by selecting and keeping the important KV-pairs only based on their similarities. The follow-up work, AdaReTaKe (Wang et al., 2025b) applies prompt-based KV-Cache selection depending on the attention scores.

2.2. Online Video Understanding and TTT

Online video understanding requires processing frames continuously in real time, where the stream length is unknown, precluding the offline practice of pre-selecting a fixed, uniformly sampled frame set. Models, therefore, must operate under a fixed memory budget to stay within the LLM’s context window. Prior work follows two main directions. Token-reduction methods fix the number of visual tokens: MovieChat (Song et al., 2024) merges tokens via similarity-based consolidation, and VideoLLMonline (Chen et al., 2024) reduces each frame to about 10 tokens for efficiency. External-memory methods compress and organise visual tokens and retrieve the most relevant ones at query time: Flash-VStream (Zhang et al., 2024a) and Dispider (Qian et al., 2025) fuse retrieved visual tokens with text tokens before feeding them into the LLM backbone. A complementary line targets KV-cache compression and retrieval: ReKV (Di et al., 2025) offloads layer-wise caches to external storage for on-demand fetching; (Ning et al., 2025) compresses the KV cache to cut memory and accelerate question answering (QA) relative to ReKV; StreamMem and InfiniPot-V (Kim et al., 2025) further improve efficiency via dynamic, non-uniform KV compression. Wang et al. (2025a) explores test-time training for video segmentation, but focuses on adaptation to local changes at test time that do not require long-term dependencies. In contrast, **video-SALMONN S** mitigates hard token dropping/merging by using TTT to continually update the memory representations, mitigating information loss while meeting a fixed memory budget.

3. video-SALMONN S Training and Test

The overall structure of video-SALMONN S is shown in Fig. 1. The input video is processed in streaming mode at a fixed frame rate, *e.g.* 1 FPS. Each video frame is first converted into video encodings using a visual encoder, followed by a pre-trained modality aligner that projects the representations to the text space, denoted as \mathbf{X}_t . Video encodings \mathbf{X}_t are then fed into the TTT_{MEM} layer, which incorporates the full sequence history into the representations. We maintain a long-term memory of a fixed number of tokens, and the output of the TTT_{MEM} layer for the current frame provides new incoming tokens to be added to the memory. Thereafter, merging or downsampling is performed to ensure a fixed number of tokens is sent to the Transformer.

In recent LLM designs, such as Qwen3-VL (Bai et al.,

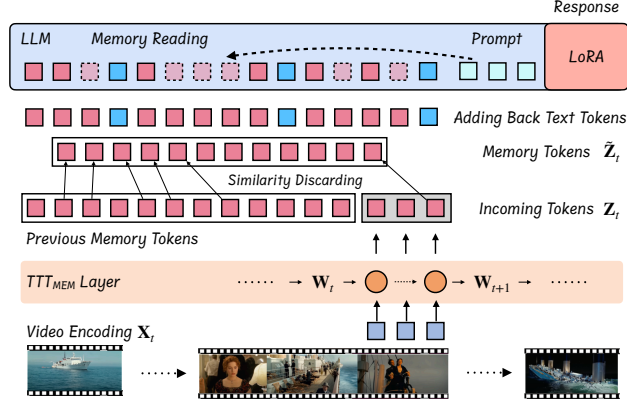


Figure 1. Overall model structure of video-SALMONN S. The video encodings are first passed through the TTT_{MEM} layer (Section 3.1), followed by a similarity discarding procedure to keep fixed-size memory. The fixed memory is then used as the input to the LLM, optionally using a modality-aware prompt-dependent reading mechanism (Section 3.3).

2025a), text and timestamp tokens are often interleaved with multimodal tokens. We use TTT_{MEM} to process multimodal tokens only, and then add those text tokens back while maintaining their original relative positions in the sequence. Besides, to enable a larger memory size while still maintain fixed GPU footprint, video-SALMONN S employs a modality-aware prompt-dependent memory reading mechanism in each Transformer block to select useful KV-cache based on attention scores. The TTT_{MEM} layer and the low-rank adapter (LoRA) contain trainable parameters, and other parts of the model are frozen throughout training.

3.1. Memory with TTT_{MEM} Layer

The long-term memory in video-SALMONN contains a TTT_{MEM} layer followed by a token discarding process to keep the total number of tokens to the Transformer constant. Specifically, given the chunk of video encodings denoted as $\mathbf{X}_t \in \mathbb{R}^{K \times d}$ where K is the number of tokens, the incoming memory token to be added to the memory is derived as

$$\mathbf{Z}_t, \mathbf{W}_t = \text{TTT}_{\text{MEM}}(\mathbf{X}_t, \mathbf{X}_{t-T}, \mathbf{W}_{t-1}), \quad (1)$$

where \mathbf{W}_{t-1} is the weight carrying history information and is updated to incorporate the information in \mathbf{X}_t as well as \mathbf{X}_{t-T} via a long-span prediction task. The gating mechanism following (Dalal et al., 2025) is used. Since audio tokens are only about 1/75 the number of visual tokens, they bypass TTT_{MEM} and are fed directly into the token discarding stage, simplifying TTT_{MEM} to visual-only inputs.

The memory tokens \mathbf{Z}_t are then combined with previous memory tokens $\tilde{\mathbf{Z}}_{t-1} \in \mathbb{R}^{N \times d}$ where N is the fixed number of memory tokens following a cosine similarity-based token discarding procedure (Song et al., 2024; Yang et al., 2025b). Specifically, let us denote $\mathbf{Z}'_t = \text{Concat}(\tilde{\mathbf{Z}}_{t-1}, \mathbf{Z}_t)$ along the sequence dimension, that is, $\mathbf{Z}'_t \in \mathbb{R}^{(N+K) \times d}$. We

discard K tokens that have the highest cosine similarities with their next tokens, *i.e.* $\cos(\mathbf{Z}'_{t,n}, \mathbf{Z}'_{t,n+1})$. The remaining N tokens become the new memory tokens, $\tilde{\mathbf{Z}}_t$. Note that we particularly chose to discard rather than the merging operation adopted in MovieChat (Song et al., 2024) to better exploit the long-term context representation ability of TTT_{MEM} layer and avoid over-smoothing in extremely long videos. Despite discarding tokens, the fast-weight state produced by TTT_{MEM} can preserve useful summaries of past inputs. The long-span objective encourages retention of information relevant across distant timestamps.

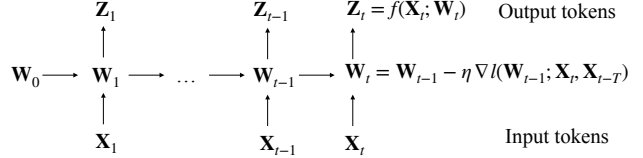


Figure 2. The workflow of the TTT_{MEM} layer. The layer works as a recurrent neural network, which updates the current fast-weight \mathbf{W}_{t-1} of an MLP model for an incoming mini-batch of tokens \mathbf{X}_t to minimise the reconstruction loss and the long-span prediction loss, which involves \mathbf{X}_{t-T} as shown in Eqn. (4).

The overall workflow is shown in Fig. 2. The TTT_{MEM} layer consists of a multi-layer perceptron (MLP) model with fast weights \mathbf{W} . We divided the entire input sequence into fixed-size chunks $\mathbf{X}_1, \mathbf{X}_2, \dots, \mathbf{X}_t, \dots$, treating them as minibatches and sending each of them in consecutive order to the TTT_{MEM} layer. Each minibatch contains around 12-16 frames. TTT_{MEM} adopts the multiview reconstruction loss and the long-span prediction loss:

$$l_{\text{recon}}(t) = \|f(\theta_{\mathbf{K}} \mathbf{X}_t; \mathbf{W}_{t-1}) - \theta_{\mathbf{V}} \mathbf{X}_t\|_2 \quad (2)$$

$$l_{\text{long-span}}(t) = \|f(\theta'_{\mathbf{K}} \mathbf{X}_t; \mathbf{W}_{t-1}) - \theta'_{\mathbf{V}} \mathbf{X}_{t-T}\|_2 \quad (3)$$

where θ are trainable projection weights and $f(\cdot; \mathbf{W})$ denotes the function of the MLP model following the residual and layer norm (LN) operation by (Dalal et al., 2025). The fast weights are trained to minimize the following:

$$l(\mathbf{X}_t, \mathbf{X}_{t-T}; \mathbf{W}_{t-1}) = l_{\text{recon}}(t) + l_{\text{long-span}}(t), \quad (4)$$

where T is a hyper-parameter determining how far we predict. While \mathbf{W}_t already incorporates information of past inputs, when the sequence becomes longer, previous information would inevitably be overwritten by new updates. The long-span prediction loss acts as a temporal consistency regularizer on the fast-weight updates, encouraging the model to maintain representations predictive of inputs from $t - T$, which improves retention over long sequences.

The fast weight can be updated with gradient descent $\mathbf{W}_t = \mathbf{W}_{t-1} - \eta \nabla l(\mathbf{X}_t, \mathbf{X}_{t-T}; \mathbf{W}_{t-1})$. The updated multilayer perceptron (MLP) is used to produce the output token \mathbf{Z}_t by

$$\mathbf{Z}_t = f(\theta_{\mathbf{Q}} \mathbf{X}_t; \mathbf{W}_t). \quad (5)$$

The name of TTT comes from the fact that the fast weight \mathbf{W}_t is updated for each incoming mini-batch at test time.

3.2. Two-Stage Training Scheme

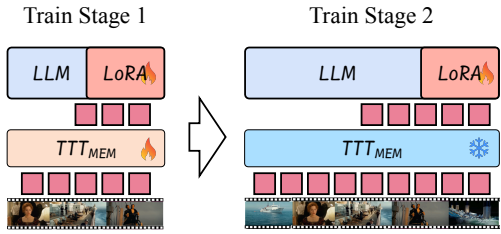


Figure 3. Illustration of the two-stage training scheme for video-SALMONN S. Stage 1 trains the entire model end-to-end with both LoRA and TTT_{MEM} parameters updated. Stage 2 scales up with longer sequences and more memory tokens by freezing TTT_{MEM} parameters while keeping the same update rule for fast weights.

One bottleneck during training is the GPU memory consumption at the TTT_{MEM} layer when the input sequence gets longer. In order to balance the training of the TTT_{MEM} model parameters, *i.e.* θ projection matrices in Eqn. (3), input lengths and memory tokens, the two-stage training scheme is adopted, as shown in Fig. 3. *Stage 1* is a cold-start stage where TTT_{MEM} parameters are randomly initialized and are jointly trained with the LLM. After stage 1, the fast weight update mechanism is established. *Stage 2* training is conducted thereafter to scale up input and memory by freezing θ in TTT_{MEM} but maintaining the fast weight update rule. This stage further optimizes the LLM to extract information from memory with much longer input sequence lengths and more memory tokens.

3.3. Modality-Aware Memory Reading

The video memory token sequence $\tilde{\mathbf{Z}} \in \mathcal{R}^{N \times d}$ after TTT_{MEM} already contains comprehensive information from the preceding video. However, when responding to a specific prompt $\mathbf{P} \in \mathcal{R}^{S \times d}$, it is usually unnecessary to utilise all memory tokens, which brings both performance issues and high computational cost. Therefore, we employ a modality-aware prompt-dependent memory reading mechanism to select only the relevant part of the memory.

We aim to leverage the LLM to compress the number of KV pairs used for final decoding to an average of M tokens per layer. Specifically, the tokens are first divided into chunks of length m , resulting in $\lceil N/m \rceil$ chunks, $\tilde{\mathbf{Z}}_i$, to reduce computational requirements. For each chunk at layer l , we concatenate the input of this chunk with prompt tokens forwarded to layer l , and apply multi-head self-attention by

$$\mathbf{O}_i^{(l)} = \text{Attention} \left([\mathbf{X}_i^{(l)}; \mathbf{X}_p^{(l)}] | \mathbf{KV}_{1:i-1}^{(l)} \right), \quad (6)$$

where $[\cdot; \cdot]$ denotes concatenation of vectors along sequence

direction, $\mathbf{X}_i^{(l)}$ are $\tilde{\mathbf{Z}}_i$ forwarded to layer l and $\mathbf{X}_p^{(l)}$ are \mathbf{P} forwarded to layer l . $\mathbf{KV}_{1:i-1}$ are compressed KV cache carried over up to chunk i . Attention $(\cdot | \cdot)$ is the standard LLM attention (Bai et al., 2025a) with KV-Cache, with $[\mathbf{X}_i^{(l)}; \mathbf{X}_p^{(l)}]$ being the input. We then compute the average attention score from the prompt to each position in chunk i to reflect the importance of each KV pair as

$$\mathbf{c}_i^{(l)} = \sum_{s=1}^S \frac{1}{H} \sum_{h=1}^H \mathbf{A}_i^{(l)}[h, s], \quad (7)$$

where $\mathbf{A}_i^{(l)}[h, s] \in \mathbb{R}^m$ is the attention score from token s to all vectors in $\mathbf{X}_i^{(l)}$ and H is the number of attention heads. We concatenate $\mathbf{c}_i^{(l)}$ with previous scores $\mathbf{c}_{1:i-1}^{(l)}$, and select a maximum of m KV pairs with the highest importance for tokens that correspond to multimodal input positions, with a mask operation as follows:

$$\mathbf{I}_i = \text{ArgTop}(\text{Mask}([\mathbf{c}_{1:i-1}^{(l)}; \mathbf{c}_i^{(l)}]), k = m) \quad (8)$$

$$\hat{\mathbf{I}}_i = \text{Sorted}([\mathbf{I}_i; \mathbf{I}_{\text{other}}]) \quad (9)$$

$$\mathbf{KV}_{1:i}^{(l)} = [\mathbf{KV}_{1:i-1}^{(l)}; \mathbf{KV}_i^{(l)}][\hat{\mathbf{I}}_i], \quad (10)$$

where $\text{Mask}(\cdot)$ is the function that selects positions corresponding to multimodal tokens, $\text{ArgTop}(\cdot, k = \cdot)$ selects the top k elements and $\text{Sorted}(\cdot)$ sorts indices in ascending order. The KV pairs corresponding to other non-multimodal tokens, $\mathbf{I}_{\text{other}}$, are added back, maintaining their relative positions unchanged, which is crucial to ensure the correct functioning of the model.

After $\lceil N/m \rceil$ iterations, all remaining KV pairs contain highly condensed content that is relevant to the current question. The LLM then generates a response based on the prompt and the extracted KV pairs. This mimics the process of extracting task-specific information from long-term memory to working memory in the human brain (Jeneson & Squire, 2012; Chai et al., 2018). Since the memory size is fixed, it still satisfies streaming constraints.

4. Episodic Learning from Video Memory

Humans often acquire skills by observing demonstrations, increasingly through short videos, and recall these skills later from long-term memory when performing similar tasks. The ELViM benchmark is designed to simulate this process by evaluating whether LLMs can learn procedural knowledge from episodic video memory and retrieve it to support real-time task execution. As illustrated in Fig. 4, a target video containing procedural information is first presented, followed by a long sequence of unrelated videos. After an extended interval, the target video is replayed and paused at a specific moment just before the demonstrator performs the next step, at which point the model is queried about the upcoming action.



Figure 4. Illustration of the ELViM data. The question is given at a specific timestamp, asking about the next step to execute. The answer can be found in the target video, which has been watched for at least 30 minutes before the time of the question.

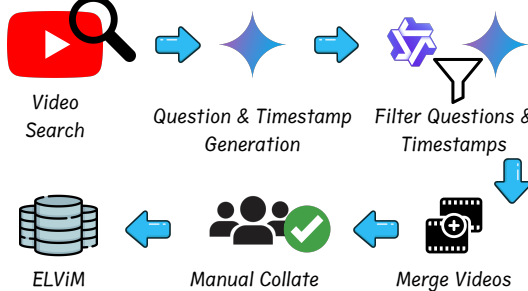


Figure 5. Data creation and annotation pipeline for ELViM.

ELViM differs from existing knowledge acquisition benchmarks such as VideoMMMU (Hu et al., 2025) in two key aspects: (i) the videos are substantially longer, lasting up to 2 hours, with the relevant knowledge appearing at least 30 minutes before the query; and (ii) questions are posed at a precise time point within an ongoing video, requiring real-time awareness of task progress. As a result, ELViM tests real-time perception and long-term memory, reflecting the requirements of future real-world agents that must acquire and reuse skills from extended audio-visual experiences.

4.1. Data Creation Pipeline

We adopt a rigorous data creation pipeline to avoid knowledge leakage or textual shortcuts, as shown in Fig. 5.

Video collection and question generation: We first collect over 1000 tutorial or demonstration videos spanning 15 categories that were uploaded after mid-2025. We then generate 10 questions about certain procedures for each video, together with their corresponding timestamps and distracting choices using Gemini-2.5-Pro.

Question and timestamp filtering: Next, we ensure the questions cannot be answered by the model’s own knowledge or inference from previous steps. We prompt Gemini-2.5-Pro and Qwen3-VL-8B with questions and video up to the timestamp when the target procedure begins. We then kept the questions that those models fail to answer with incomplete videos, but can answer with complete ones.

Rest of the steps: At last, we concatenate single videos into long merged videos, each up to 90 minutes, where the target video is at least 30 minutes away from the question timestamp. Thereafter, human collation is performed for the correctness of the question and the accuracy of the times-

tamp in the merged video. We provide detailed statistics of the ELViM dataset as well as the detailed performance on single videos in Appendix A. Example questions and answers are provided in Appendix B.

5. Experimental Setup

5.1. Model

video-SALMONN S is built based on the Qwen3-VL 8B backbone (Bai et al., 2025a). Following video-SALMONN-2 (Tang et al., 2025a), Whisper-Large-v3 encoder (Radford et al., 2023) is used to encode audio information and a window-level Q-Former with a window length of 0.5 seconds as the audio aligner. The LLM backbone is trained with LoRA using a rank of 128. Without memory reading, we experiment with 16k memory tokens with 1k tokens allocated for real-time perception. With memory reading, we double the amount of memory tokens with a chunk size of 8k, so that the GPU memory is similar to 16k tokens.

TTT_{MEM} contains 2 fully-connected layers with GeLU activation function. The input encoding is converted into 8 heads, where each head is 512-dimensional and is handled by one fast weight, yielding sixteen 512×512 fast weights. The trainable learning rate η follows the same setting as (Dalal et al., 2025). We use stochastic gradient descent with one update step for TTT_{MEM} . We set $T = 2$ as the default for long-span prediction, and experimented with T ranging from 1 to 32 as shown in Table 10 in Appendix G. Detailed FLOP statistics of TTT_{MEM} and base models are provided in Appendix D. As a design choice for Qwen3-VL, deepstack embeddings are directly discarded according to the indices at the output of TTT_{MEM} without additional TTT_{MEM} , based on the results in Appendix E.

5.2. Training Configurations

Following (Tang et al., 2025a), the audio aligner of video-SALMONN S is first trained using LibriSpeech 960-hour (Panayotov et al., 2015), CommonVoice (Ardila et al., 2020), WavCaps (Mei et al., 2024), and AudioCaps (Kim et al., 2019), with other parts of the LLM frozen. Then, FineVideo (Farré et al., 2024), CinePile (Rawal et al., 2024), and about 100k videos sampled from LLaVA-Video-178k are used to finetune the entire audio-visual model following the two-stage training scheme.

During stage 1 training, we use a 4 FPS sampling rate with a maximum of 1024 frames in total to achieve a better trade-off between parallelisation and sequence lengths. The first stage trains for 3 epochs with a learning rate of 2×10^{-5} , which takes 48 hours on $32 \times$ H800 GPUs. In stage 2 training, we increase the number of frames to 2048 and train for another epoch, which takes 16 hours on $32 \times$ H800 GPUs. We use 1 sample per minibatch on one GPU.

5.3. Evaluation Configurations

Following recent studies of memory in streaming models (Yang et al., 2025a; Zeng et al., 2025), we evaluate video-SALMONN S on both general long video benchmarks, where the system operates in streaming mode, as well as streaming-specific benchmarks with long videos.

Benchmarks: For long video benchmarks, we use **Video-MME** (Fu et al., 2024) which contains several minutes to 1 hour videos. We also include **LBench** and **VideoEvalPro** as two extremely long video QA benchmarks. LBench (Wang et al., 2024b) contains videos of several hours that focus on long-term memory and diverse core capabilities, and VideoEvalPro (Ma et al., 2025) also contains videos of several hours, and is designed to more realistically evaluate long video understanding without MCQ shortcuts, where the MCQ partition is used. For streaming-specific benchmarks, we primarily compare systems on our proposed **ELViM** benchmark, and at the same time evaluate on **StreamingBench** (Lin et al., 2024a). Note that StreamingBench does not contain long videos where long-term memory is necessary. The experiments are mainly to demonstrate the state-of-the-art performance of video-SALMONN S on standard online video tasks. Percentage accuracies are reported on all these benchmarks.

Baselines: We employ 2 streaming baselines for our experiments, including memory consolidation (Song et al., 2024; Chen et al., 2024) and Persistent event memory forest (PEMF) in StreamForest (Zeng et al., 2025)². We implement the memory algorithms in each of the baselines in our model to ensure they have the same backbone LLM and the same training data. We also compare with strong non-streaming baselines, including Qwen3-VL itself and video-SALMONN 2 (Tang et al., 2025a). Regarding the reading mechanism, we compare with AdaReTaKe (Wang et al., 2025b) on the same model.

For streaming models, the video is processed at 1 FPS by default, and has an alternative 4 FPS for videos less than 2 minutes (*i.e.* exclusively used for Video-MME short partition). For non-streaming models, we use up to 10 FPS sampling rate and apply a maximum token limit of 16k, and

²Due to the large number of visual tokens, we compute penalty and perform merging on-the-fly for every 64 incoming frames

uniformly sample frames when exceeding the limit.³

6. Results

6.1. Main Results

We first present the main results in Table 1, where video-SALMONN S operates under an effective memory budget of 16k memory tokens corresponding to 215 input video frames for non-streaming models, and ~ 24 GB GPU memory, respectively. Note that all systems in Table 1 are based on the same LLM backbone and the same training data, and hence they only differ in how the long-term memory is constructed. For PEMF, we use the default penalty coefficients (0.4, 0.4, 0.2) from the original paper.

Overall, **video-SALMONN achieved the best performance** on standard long video benchmarks compared to both streaming and non-streaming baselines. Specifically, with 16k memory tokens compared to its non-streaming counterpart, video-SALMONN S achieved 1.7%, 2.9% and 5.4% accuracy improvements with 16k memory tokens on Video-MME long, LBench and VideoEvalPro, respectively. This advantage further increases compared to the streaming counterparts, with 1.9%, 4.0% and 7.1% absolute accuracy improvements. Such large gains achieved by video-SALMONN S demonstrate its superior long-term memory design. On StreamingBench, where long-term memory is not critical, video-SALMONN S still achieves competitive performance in real-time perception tasks.

With 80GB memory GPUs, we could further increase the number of memory tokens, and we provide results when using 128k memory in Appendix F to show the extreme case on a single GPU. Note that with this memory size, videos less than 30 minutes at 1 FPS do not need any merging or token compression, and hence we should focus on the results on longer benchmarks.

Moreover, **video-SALMONN S achieved significantly better performance on ELViM** compared to baselines. For non-streaming baselines, sparse frame sampling may omit the target video in history, as well as omit the real-time perception of the current progress, therefore leading to the worst performance overall. Similarity merging and PEMF, on the contrary, maintain good real-time perception abilities and hence perform better than the non-streaming baseline. However, both streaming methods suffer from long-term memory, so even if they correctly perceive the progress, they struggle to find the correct answer to it.

This is also reflected by the performance differences of PEMF and similarity merging on StreamingBench and long video benchmarks. Our observation on Video-MME and

³Code implementation of video-SALMONN S and ELViM questions are provided in the supplementary material.

Table 1. Performance of video-SALMONN S on various benchmarks compared against baselines. Numbers are all percentage accuracies. The short, medium and long partitions (S/M/L) are reported separately for Video-MME, and the real-time, omni-modal and contextual partitions (R/O/C) are reported for StreamingBench. Note that all baseline methods are implemented using the same Qwen3-VL base and the same training data, which are all *better* than the reported numbers in original papers.

Model	Video-MME (S/M/L)	LVBenchmark	VideoEvalPro	ELViM	StreamingBench (R/O/C)
Effective memory budget 16k memory tokens					
Qwen3-VL 8B (Bai et al., 2025a)	69.7 (80.7/68.3/60.1)	47.4	54.9	28.1	61.8 (76.9/42.5/37.5)
video-SALMONN 2+ (Tang et al., 2025a)	75.6 (81.6/75.7/69.6)	52.7	53.5	32.5	66.4 (77.7/57.5/41.0)
Similarity Merging (Song et al., 2024)	75.8 (82.0/76.2/69.4)	51.6	51.8	38.5	66.8 (78.1/59.5/39.2)
PEMF (Zeng et al., 2025)	75.8 (82.7/76.1/68.6)	49.5	50.4	38.2	67.1 (79.1/57.1/40.8)
video-SALMONN S (w/o reading)	76.4 (82.7/75.2/71.3)	55.4	55.8	43.9	66.8 (78.4/57.5/40.9)
video-SALMONN S (w reading)	76.9 (82.5/76.8/71.3)	55.6	58.9	46.7	67.1 (78.9/57.5/41.5)

StreamingBench generally aligns with the original paper (Zeng et al., 2025). While similarity merging and PEMF perform well on short to medium-length videos, their performances degrade on videos of 3-4 hours in length. The differences between PEMF and similarity merging on LVBenchmark and VideoEvalPro are mainly due to the temporal penalty. In contrast, TTT_{MEM} achieves a better balance by incorporating both near and far history information into fast weights. As a result, video-SALMONN S achieves 14.2% improvements compared to the non-streaming baseline, and 8.8% to PEMF with 16k memory tokens. Qualitative case studies are provided in Appendix C to further support our claims.

6.2. Ablation Studies

We provide **the contribution of different design choices in video-SALMONN S** in Table 2. First, we compare different downsampling techniques, including merging, clustering and discarding. We observe that merging and discarding achieved similar performance, that are both superior to clustering of tokens. Then, we compare the effect of TTT_{MEM} against TTT-video⁴ and Mamba 2 as two alternative RNN-type long-term memory mechanisms. We observe that TTT-video achieved consistently better performance than Mamba 2 in long video understanding. TTT_{MEM} further improves the performance of TTT-video by 1-2%, which is mainly due to the newly introduced long-span prediction loss. The second stage training further improves long video understanding by 0.2-0.4%, with a modest effect on relatively short videos such as Video-MME long.

The comparison between AdaReTaKe (Wang et al., 2025b), a recent training-free KV-Cache compression method, and our proposed reading mechanism is also performed. As shown in Table 2, our modality-aware reading mechanism achieved consistent and significant performance improvements compared to AdaReTaKe.

Influence of memory size: The variation of long-term mem-

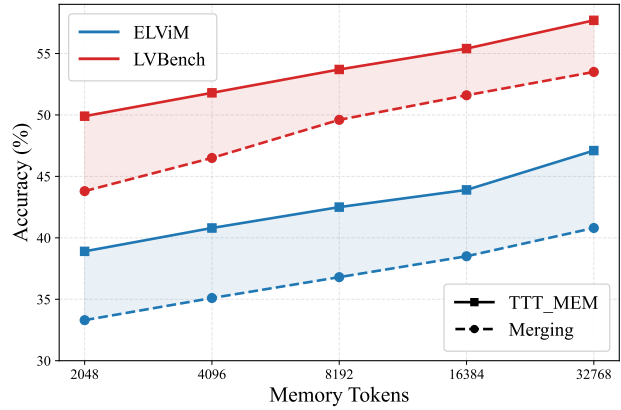


Figure 6. Model performance against different numbers of memory tokens on ELViM and LVBenchmark using merging and TTT_{MEM} without reading mechanism. TTT_{MEM} achieves the same level of accuracy with less than 25% of memory tokens needed by merging.

ory performance on ELViM and LVBenchmark against different memory sizes is shown in Fig. 6. Note that memory reading is not used, so that the comparison is purely focused on the two long-term memory mechanisms. Overall, TTT_{MEM} shows a more robust trend than Merging when the number of memory tokens reduces to 4k and 2k, and maintains its advantage across all different memory sizes we evaluated. Notably, on both datasets, TTT_{MEM} achieves similar accuracies as merging baselines with only equal to or less than 25% of memory tokens used by merging, demonstrating its strong long-term memory capability.

Influence of number of frames: The performance change against increasing number of input frames on ELViM and LVBenchmark is shown in Fig. 7, with 16k memory token budget for both methods. Again, the reading mechanism is excluded to focus on long-term memory mechanisms. While both methods show an upward trend when the number of frames increases from 256 to 2048, the similarity merging method suffers significantly when the number of frames continues to grow exponentially. On the contrary, TTT_{MEM} shows a steady upward trend up to 4096 frames, and reaches

⁴TTT-video refers to the standard TTT in (Dalal et al., 2025).

Table 2. Ablation studies on different components in video-SALMONN S with 16k memory token settings on long video benchmarks without memory reading. “Reading” refers to our proposed modality-aware reading mechanism.

Configuration	Video-MME Long	LVBench	VideoEvalPro	ELViM
Similarity Merging (Song et al., 2024)	69.4	51.6	51.8	35.4
K-means Clustering (Zhou et al., 2024)	67.8	49.8	50.7	33.8
Similarity Discarding	69.2	51.1	51.5	36.8
+ Mamba-2 (Dao & Gu, 2024)	70.3	53.5	54.8	39.6
+ TTT-video (Datal et al., 2025)	70.0	54.3	54.9	42.3
+ TTT _{MEM} w/o Stage 2 Training	71.3	55.1	55.5	43.6
+ Stage 2 Training (video-SALMONN S w/o reading)	71.3	55.4	55.8	43.9
video-SALMONN S + AdaReTaKe (Wang et al., 2025b)	70.8	55.1	56.5	43.6
video-SALMONN S + Reading	71.3	55.6	58.9	46.7

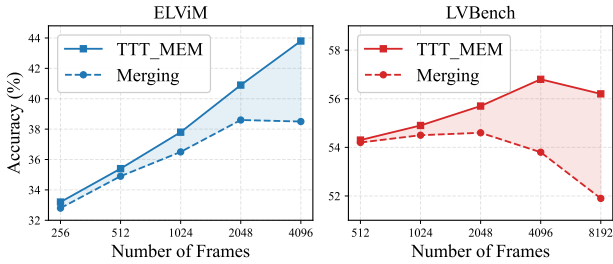


Figure 7. Variation of model performance against different numbers of input frames on ELViM and LVBench using similarity merging and TTT_{MEM} without the reading mechanism. Both methods use 16k memory tokens. The X-axis is on a log scale.

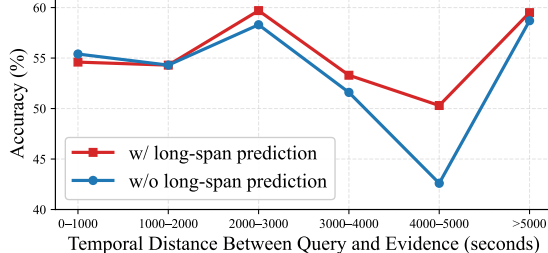


Figure 8. Comparison of video-SALMONN S with and without long-span prediction on LVBench at different temporal distances between the query and evidence.

the plateau after that without obvious degradation. The onset of the plateau is determined by the number of memory tokens budget, and can be significantly postponed to over 10k frames using 32k memory tokens.

Influence of long-span prediction: Since LVBench also provides the time at which the answer could be found in the video, we plot the model performance against the temporal distance between the evidence location and the query time in Fig. 8. We compare TTT_{MEM} with and without long-span prediction in this plot to demonstrate that the long-span prediction helps to retain information. Long-span prediction yields consistent improvements as the temporal distance between the query and evidence increases, demonstrating its effectiveness in modeling long-term dependencies.

6.3. Runtime Statistics

Table 3. Memory and inference time per sample measured for Video-MME long at 1 FPS (maximum 3600 frames) on a single H800 GPU with 16k memory tokens.

Model	GPU Mem. (Avg./Peak)	Infer. Time (second)
Similarity Merging	21.9 / 24.1	10.4
PEMF	21.9 / 24.1	10.4
v-SALMONN S (w/o Reading)	22.2 / 24.3	10.5
v-SALMONN S (w/ Reading)	22.5 / 24.4	10.9

We compare runtime statistics among different streaming methods as shown in Table 3, with the same number of input frames. All models consumes similar amount of GPU memory. The inference time is the time taken from inputting the video to generating the entire answer, which is around 10 seconds. Most of the time is spent on encoding visual inputs, as there are far more frames to deal with than short videos. However, the average time taken for each frame is very short, and this can be done on-the-fly. TTT_{MEM} only creates 0.1s overhead on top of this. Reading mechanism costs another 0.4s due to the iterative prefill of token chunks into KV-Cache in Transformer.

7. Conclusion

In this paper, we propose video-SALMONN S, a memory-enhanced video LLM that processes over 3-hour videos at 1 FPS and 360p resolution. video-SALMONN S is the first to explore test-time training in long-term memory modeling. We include novel components, including a long-span prediction objective, a two-stage training pipeline and a modality-aware memory reading mechanism. In addition, we propose an episodic learning from video memory (ELViM) benchmark, which tests whether LLMs can learn from past experiences and apply them to real-time tasks. Consistent and significant improvements compared to both streaming and non-streaming baselines were achieved on a range of long video benchmarks. Notably, a 14.2% absolute accuracy improvement was achieved on ELViM.

Impact Statement

This work introduces video-SALMONN-S, a memory-enhanced streaming audio-visual large language model designed to process long-duration videos under fixed memory constraints. By enabling models to consolidate information from hours-long video streams and recall it when needed, this research advances the development of AI systems that can learn from extended experience, a capability that is important for future assistive agents, educational tools, and long-horizon decision-making systems.

The proposed approach may benefit applications such as instructional assistance, long-form educational video understanding, human-computer interaction, and support for users who rely on audio-visual information over extended periods (e.g., accessibility tools for visually or cognitively impaired users). The introduced ELViM benchmark may also encourage more rigorous evaluation of long-term memory and continual learning in multimodal systems, contributing to more transparent and realistic assessment practices in the research community.

Models capable of long-term memory accumulation from video streams could raise privacy concerns if deployed on sensitive or personal video data without appropriate safeguards. There is also a risk that long-term memory mechanisms may inadvertently encode biased, misleading, or harmful content observed in training or deployment environments, potentially amplifying such information over time. Additionally, the computational and energy costs associated with large multimodal models may contribute to environmental impacts if deployed at scale.

These risks can be mitigated through careful dataset curation, deployment-time privacy controls, explicit user consent for long-term memory storage, and mechanisms for memory inspection, reset, or forgetting. Bias and safety auditing should be applied to both training data and downstream deployments, particularly in agent-like scenarios. From a systems perspective, continued work on efficiency and memory-constrained operation, as explored in this paper, can help reduce unnecessary computational overhead.

References

Ardila, R., Branson, M., Davis, K., Kohler, M., Meyer, J., Henretty, M., Morais, R., Saunders, L., Tyers, F., and Weber, G. Common Voice: A massively-multilingual speech corpus. In *Proc. LREC*, 2020.

Bai, S., Cai, Y., Chen, R., Chen, K., Chen, X., Cheng, Z., Deng, L., Ding, W., Gao, C., Ge, C., Ge, W., Guo, Z., Huang, Q., Huang, J., Huang, F., Hui, B., Jiang, S., Li, Z., Li, M., Li, M., Li, K., Lin, Z., Lin, J., Liu, X., Liu, J., Liu, C., Liu, Y., Liu, D., Liu, S., Lu, D., Luo, R., Lv, C., Men, R., Meng, L., Ren, X., Ren, X., Song, S., Sun, Y., Tang, J., Tu, J., Wan, J., Wang, P., Wang, P., Wang, Q., Wang, Y., Xie, T., Xu, Y., Xu, H., Xu, J., Yang, Z., Yang, M., Yang, J., Yang, A., Yu, B., Zhang, F., Zhang, H., Zhang, X., Zheng, B., Zhong, H., Zhou, J., Zhou, F., Zhou, J., Zhu, Y., and Zhu, K. Qwen3-VL Technical Report. *arXiv:2511.21631*, 2025a.

Bai, S., Chen, K., Liu, X., Wang, J., Ge, W., Song, S., Dang, K., Wang, P., Wang, S., Tang, J., Zhong, H., Zhu, Y., Yang, M., Li, Z., Wan, J., Wang, P., Ding, W., Fu, Z., Xu, Y., Ye, J., Zhang, X., Xie, T., Cheng, Z., Zhang, H., Yang, Z., Xu, H., and Lin, J. Qwen2.5-VL Technical Report. *arXiv:2502.13923*, 2025b.

Chai, W. J., Abd Hamid, A. R., and Abdullah, J. M. Working memory from the psychological and neurosciences perspectives: A review. *Frontiers in Psychology*, 9:401, 2018.

Chen, J., Lv, Z., Wu, S., Lin, K. Q., Song, C., Gao, D., Liu, J.-W., Gao, Z., Mao, D., and Shou, M. Z. VideoLLM-online: Online video large language model for streaming video. In *Proc. CVPR*, 2024.

Dalal, K., Koceja, D., Hussein, G., Xu, J., Zhao, Y., Song, Y., Han, S., Cheung, K. C., Kautz, J., Guestrin, C., Hashimoto, T., Koyejo, S., Choi, Y., Sun, Y., and Wang, X. One-minute video generation with test-time training. In *Proc. CVPR*, 2025.

Dao, T. and Gu, A. Transformers are SSMs: Generalized models and efficient algorithms through structured state space duality. In *Proc. ICML*, 2024.

Di, S., Yu, Z., Zhang, G., Li, H., Zhong, T., Cheng, H., Li, B., He, W., Shu, F., and Jiang, H. Streaming video question-answering with in-context video kv-cache retrieval. *arXiv preprint arXiv:2503.00540*, 2025.

Farré, M., Marafioti, A., Tunstall, L., von Werra, L., and Wolf, T. Finevideo. <https://huggingface.co/datasets/HuggingFaceFV/finevideo>, 2024. Accessed: 2025-09-17.

Fu, C., Dai, Y., Luo, Y., Li, L., Ren, S., Zhang, R., Wang, Z., Zhou, C., Shen, Y., Zhang, M., Chen, P., Yanwei, L., Shaohui, L., Sirui, Z., Ke, L., Tong, X., Xiawu, Z., Enhong, C., Rongrong, J., and Xing, S. Video-MME: The first-ever comprehensive evaluation benchmark of multi-modal LLMs in video analysis. *arXiv:2405.21075*, 2024.

Gao, L., Zhong, Y., Zeng, Y., Tan, H., Li, D., and Zhao, Z. Linvt: Empower your image-level large language model to understand videos. *arXiv preprint arXiv:2412.05185*, 2024.

Hu, K., Wu, P., Pu, F., Xiao, W., Zhang, Y., Yue, X., Li, B., and Liu, Z. Video-MMMU: Evaluating knowledge acquisition from multi-discipline professional videos. *arXiv:2501.13826*, 2025.

Huang, Z., Li, X., Li, J., Wang, J., Zeng, X., Liang, C., Wu, T., Chen, X., Li, L., and Wang, L. Online video understanding: OVBNch and VideoChat-Online. In *Proc. CVPR*, 2025.

Jeneson, A. and Squire, L. R. Working memory, long-term memory, and medial temporal lobe. *Journal of Neuroscience*, 32:13325–13336, 2012.

Kim, C. D., Kim, B., Lee, H., and Kim, G. Audiocaps: Generating captions for audios in the wild. In *Proc. NAACL-HLT*, 2019.

Kim, M., Shim, K., Choi, J., and Chang, S. InfiniPot-V: Memory-constrained kv cache compression for streaming video understanding. *arXiv:2506.15745*, 2025.

Li, B., Zhang, Y., Guo, D., Zhang, R., Li, F., Zhang, H., Zhang, K., Zhang, P., Li, Y., Liu, Z., et al. Llava-OneVision: Easy visual task transfer. *arXiv preprint arXiv:2408.03326*, 2024.

Li, Y., Tang, C., Zhuang, J., Yang, Y., Sun, G., Li, W., Ma, Z., and Zhang, C. Improving LLM video understanding with 16 frames per second. In *Proc. ICML*, 2025.

Lin, J., Fang, Z., Chen, C., Wan, Z., Luo, F., Li, P., Liu, Y., and Sun, M. Streamingbench: Assessing the gap for mllms to achieve streaming video understanding. *arXiv preprint arXiv:2411.03628*, 2024a.

Lin, J., Yin, H., Ping, W., Molchanov, P., Shoeybi, M., and Han, S. VILA: On pre-training for visual language models. In *Proc. CVPR*, Seattle, 2024b.

Liu, X., Shu, Y., Liu, Z., Li, A., Tian, Y., and Zhao, B. Video-XL-Pro: Reconstructive token compression for extremely long video understanding. *arXiv preprint arXiv:2503.18478*, 2025a.

Liu, X., Wang, Y., Ma, J., and Zhang, L. Video compression commander: Plug-and-play inference acceleration for video large language models. *arXiv preprint arXiv:2505.14454*, 2025b.

Long, L., He, Y., Ye, W., Pan, Y., Lin, Y., Li, H., Zhao, J., and Li, W. Seeing, listening, remembering, and reasoning: A multimodal agent with long-term memory. *arXiv:2508.09736*, 2025.

Ma, W., Ren, W., Jia, Y., Li, Z., Nie, P., Zhang, G., and Chen, W. Videoeval-pro: Robust and realistic long video understanding evaluation. *arXiv:2505.14640*, 2025.

Mei, X., Meng, C., Liu, H., Kong, Q., Ko, T., Zhao, C., Plumbley, M. D., Zou, Y., and Wang, W. WavCaps: A Chatgpt-Assisted Weakly-Labelled Audio Captioning Dataset for Audio-Language Multimodal Research. *IEE Transactions on Audio, Speech and Language Processing*, 32:3339–3354, 2024.

Ning, Z., Liu, G., Jin, Q., Ding, W., Guo, M., and Zhao, J. LiveVLM: Efficient online video understanding via streaming-oriented KV cache and retrieval. *arXiv preprint arXiv:2505.15269*, 2025.

Panayotov, V., Chen, G., Povey, D., and Khudanpur, S. Librispeech: An ASR corpus based on public domain audio books. In *Proc. ICASSP*, 2015.

Qian, R., Ding, S., Dong, X., Zhang, P., Zang, Y., Cao, Y., Lin, D., and Wang, J. Dispider: Enabling video LLMs with active real-time interaction via disentangled perception, decision, and reaction. In *Proc. CVPR*, 2025.

Radford, A., Kim, J. W., Xu, T., Brockman, G., McLeavey, C., and Sutskever, I. Robust speech recognition via large-scale weak supervision. In *Proc. ICML*, 2023.

Rawal, R., Saifullah, K., Basri, R., Jacobs, D., Somepalli, G., and Goldstein, T. Cinepile: A long video question answering dataset and benchmark. *arXiv:2405.08813*, 2024.

Shen, X., Xiong, Y., Zhao, C., Wu, L., Chen, J., Zhu, C., Liu, Z., Xiao, F., Varadarajan, B., Bordes, F., Liu, Z., Xu, H., J. Kim, H., Soran, B., Krishnamoorthi, R., Elhoseiny, M., and Chandra, V. LongVU: Spatiotemporal adaptive compression for long video-language understanding. *arXiv:2410.17434*, 2024.

Shu, Y., Zhang, P., Liu, Z., Qin, M., Zhou, J., Huang, T., and Zhao, B. Video-XL: Extra-long vision language model for hour-scale video understanding. *arXiv preprint arXiv:2409.14485*, 2024.

Song, E., Chai, W., Wang, G., Zhang, Y., Zhou, H., Wu, F., Chi, H., Guo, X., Ye, T., Zhang, Y., Lu, Y., Hwang, J.-N., and Wang, G. MovieChat: From dense token to sparse memory for long video understanding. In *Proc. CVPR*, 2024.

Sun, G., Yang, Y., Zhuang, J., Tang, C., Li, Y., Li, W., MA, Z., and Zhang, C. video-SALMONN-o1: Reasoning-enhanced audio-visual large language model. In *Proc. ICML*, 2025.

Sun, Y., Li, X., Dalal, K., Xu, J., Vikram, A., Zhang, G., Dubois, Y., Chen, X., Wang, X., Koyejo, S., Hashimoto, T., and Guestrin, C. Learning to (learn at test time): RNNs with expressive hidden states. *arXiv:2407.04620*, 2024.

Tan, R., Sun, X., Hu, P., hsien Wang, J., Deilamsalehy, H., Plummer, B. A., Russell, B., and Saenko, K. Koala: Key frame-conditioned long video-LLM. In *Proc. CVPR*, 2024.

Tang, C., Li, Y., Yang, Y., Zhuang, J., Sun, G., Li, W., Ma, Z., and Zhang, C. video-SALMONN 2: Captioning-enhanced audio-visual large language models. *arXiv:2506.15220*, 2025a.

Tang, X., Qiu, J., Xie, L., Tian, Y., Jiao, J., and Ye, Q. Adaptive keyframe sampling for long video understanding. In *Proc. CVPR*, 2025b.

Wang, P., Bai, S., Tan, S., Wang, S., Fan, Z., Bai, J., Chen, K., Liu, X., Wang, J., Ge, W., et al. Qwen2-VL: Enhancing vision-language model's perception of the world at any resolution. *arXiv preprint arXiv:2409.12191*, 2024a.

Wang, R., Sun, Y., Tandon, A., Gandelsman, Y., Chen, X., Efros, A. A., and Wang, X. Test-time training on video streams. *arXiv:2307.05014*, 2025a.

Wang, W., He, Z., Hong, W., Cheng, Y., Zhang, X., Qi, J., Huang, S., Xu, B., Dong, Y., Ding, M., and Tang, J. LVBench: An extreme long video understanding benchmark. *arXiv:2406.08035*, 2024b.

Wang, X., Si, Q., Wu, J., Zhu, S., Cao, L., and Nie, L. ReTaKe: Reducing Temporal and Knowledge Redundancy for Long Video Understanding. *arXiv:2412.20504*, 2024c.

Wang, X., Si, Q., Wu, J., Zhu, S., Cao, L., and Nie, L. AdaReTaKe: Adaptive redundancy reduction to perceive longer for video-language understanding. *arXiv preprint arXiv:2503.12559*, 2025b.

Yang, S., Yang, J., Huang, P., Brown, E., Yang, Z., Yu, Y., Tong, S., Zheng, Z., Xu, Y., Wang, M., Lu, D., Fergus, R., LeCun, Y., Fei-Fei, L., and Xie, S. Cambrian-s: Towards spatial supersensing in video. *arXiv:2511.04670*, 2025a.

Yang, Y., Zhao, Z., Shukla, S. N., Singh, A., Mishra, S. K., Zhang, L., and Ren, M. StreamMem: Query-agnostic KV cache memory for streaming video understanding. *arXiv:2508.15717*, 2025b.

Zeng, X., Qiu, K., Zhang, Q., Li, X., Wang, J., Li, J., Yan, Z., Tian, K., Tian, M., Zhao, X., Wang, Y., and Wang, L. StreamForest: Efficient online video understanding with persistent event memory. In *Proc. NeurIPS*, 2025.

Zhang, B., Li, K., Cheng, Z., Hu, Z., Yuan, Y., Chen, G., Leng, S., Jiang, Y., Zhang, H., Li, X., Jin, P., Zhang, W., Wang, F., Bing, L., and Zhao, D. VideoLLaMA 3: Frontier multimodal foundation models for image and video understanding. *arXiv preprint arXiv:2501.13106*, 2025a.

Zhang, H., Wang, Y., Tang, Y., Liu, Y., Feng, J., Dai, J., and Jin, X. Flash-vstream: Memory-based real-time understanding for long video streams. *arXiv preprint arXiv:2406.08085*, 2024a.

Zhang, H., Wang, Y., Tang, Y., Liu, Y., Feng, J., Dai, J., and Jin, X. Flash-VStream: Memory-based real-time understanding for long video streams. In *Proc. ICCV*, 2025b.

Zhang, P., Zhang, K., Li, B., Zeng, G., Yang, J., Zhang, Y., Wang, Z., Tan, H., Li, C., and Liu, Z. Long context transfer from language to vision. *arXiv preprint arXiv:2406.16852*, 2024b.

Zhang, S., Fang, Q., Yang, Z., and Feng, Y. Llava-mini: Efficient image and video large multimodal models with one vision token. In *Proc. ICLR*, 2025c.

Zhang, Y., Wu, J., Li, W., Li, B., Ma, Z., Liu, Z., and Li, C. Video instruction tuning with synthetic Data. *arXiv preprint arXiv:2410.02713*, 2024c.

Zhang, Y., Zhao, Z., Chen, Z., Ding, Z., Yang, X., and Sun, Y. Beyond training: Dynamic token merging for zero-shot video understanding. *arXiv preprint arXiv:2411.14401*, 2024d.

Zhou, X., Arnab, A., Buch, S., Yan, S., Myers, A., Xiong, X., Nagrani, A., and Schmid, C. Streaming dense video captioning. In *Proc. CVPR*, 2024.

A. ELViM Detailed Statistics

We provide descriptive statistics of ELViM in Table 4, including the number of questions, the number of videos and duration statistics of the merged videos. We also provide the distribution of categories used ELViM in Table 5. Note that some of the search queries are generic, but the actual tutorials or procedures differ greatly from video to video.

Table 4. Statistics of ELViM dataset.

Number of Questions	Number of Target Videos	Durations (Average/Max/Min)
1849	1021	2920s / 5518s / 1822s

Table 5. Category distribution of ELViM dataset.

Category	Number of target videos	Example search queries
Home repair	68	How to replace a showerhead without leaks Replace window screen mesh walkthrough
Car & bike maintenance	59	How to align bike brakes tutorial Flush car coolant step by step
Cooking fundamentals	94	How to sharpen kitchen knives with stone Scrambled eggs creamy technique tutorial
Baking & desserts	80	How to make choux pastry beginner guide Why cookies spread too much, troubleshooting
Tech help	124	Bluetooth connection issues troubleshooting Phishing email identification guide
Software skills	45	Notion task management setup guide Photoshop crop and straighten tutorial
Money & admin life skills	56	Understand insurance deductible explained How to choose a savings account
Cleaning & home organization	84	Spring cleaning whole house checklist Organize paperwork at home
Sewing & clothing repair	42	Adjust waistband size tutorial Hand sew invisible stitch tutorial
DIY crafts & maker skills	67	3D printing filament types explained Hand tool woodworking starter skills
Gardening & plants	64	Prune houseplants beginner guide How to stake plants properly
Outdoors & practical skills	67	Pack a backpack efficiently tutorial Identify animal tracks beginner guide
Communication & career skills	54	Set boundaries at work tutorial How to say no professionally
Fitness skills	70	Proper breathing during exercise Balance exercises for beginners
Art & creative skills	47	Gesture drawing beginner exercises Camera movement techniques explained

The data creation pipeline guarantees that the videos are not seen in the training set by Gemini-2.5-Pro and Qwen3-VL. As shown in Table 6, at the time when the question is asked, without having watched the video, both Qwen3-VL and Gemini-2.5-Pro produced an accuracy that is close to random guessing. With the entire video provided, both models can achieve an accuracy close to 100%, up to some visual perception errors.

Table 6. Performance of Gemini-2.5-Pro and Qwen3-VL 8B on ELViM questions with single videos.

Model	Setup	Accuracy
Qwen3-VL 8B	Video up to question timestamp	22.6%
Qwen3-VL 8B	Full video	98.7%
Gemini-2.5-Pro	Video up to question timestamp	23.5%
Gemini-2.5-Pro	Full video	99.3%

B. ELViM Examples

We provide six example questions of ELViM as shown in Fig. 9. The first example is a video demonstrating how to use a specific software, and about 1 second after the last frame shown, the demonstrator moves the cursor to the left menu to download the software. The second video demonstrates how to cook something. The question asks about the specific requirements of the machine shown in the white box in the last couple of frames. This is explained immediately in 2-3 seconds by the demonstrator. This question requires the model to understand what it means by “the machine” that appears at the moment, and associate with its memory about what the requirements for the machine are. The rest of the examples follow a similar design to the above two types.

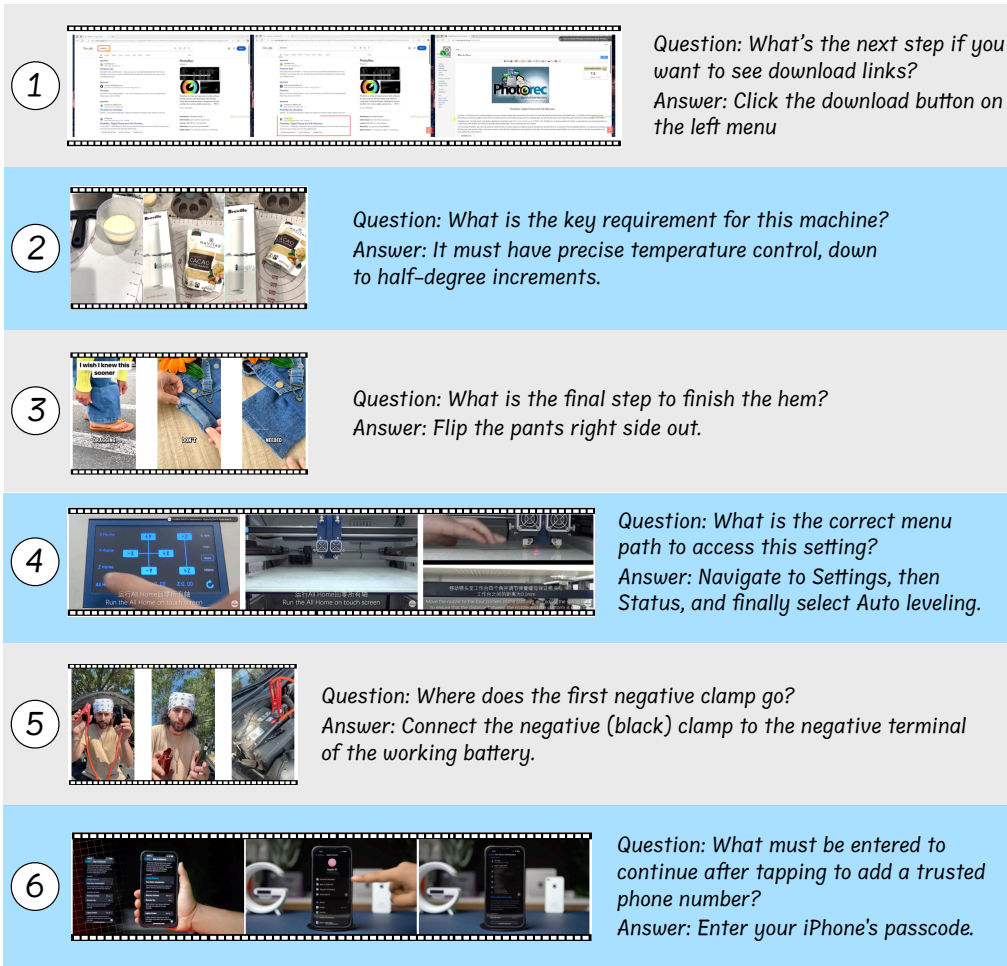
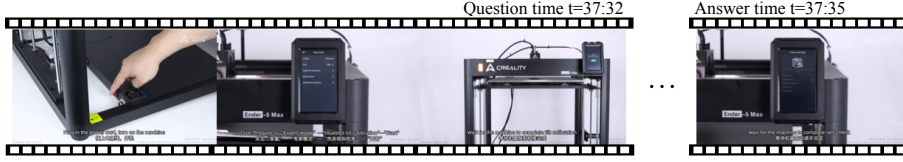


Figure 9. Examples of questions and answers in ELViM. The categories of these examples are: (1) Software skills; (2) Baking and dessert; (3) Sewing and clothing repair; (4) Tech help; (5) DIY crafts and maker skills; (6) Money and admin life skills.

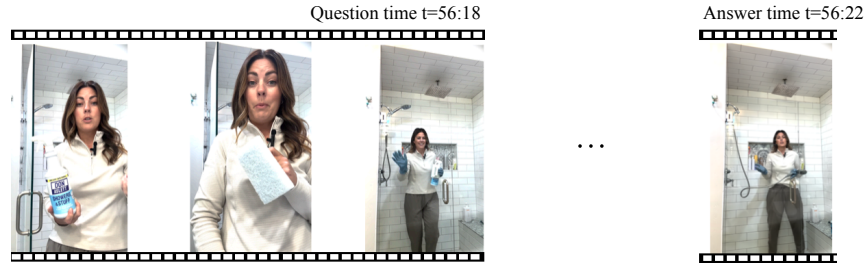
C. Qualitative Analysis on ELViM

We provide case studies on ELViM and compare the responses from different models to questions in ELViM. We convert the question into open-ended questions and let the model generate freely without giving it choices. Three examples are provided in Fig. 10 to 12 respectively.



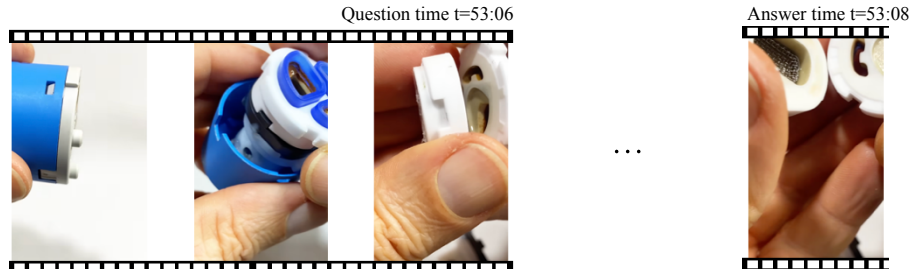
Question: What is the recommended next action after calibration?
 Reference: Perform auto-leveling and wait for self-check to complete
 Non-streaming: Checking calibration results
 PEMF: Press the button on the screen for the next step
 video-SALMONN S: Press the green button and wait for self-check to complete

Figure 10. Case study on non-streaming model, PEMF and video-SALMONN S in response to questions from ELViM. In this example, the non-streaming model fails to understand the current status of the video and hence makes an educated guess based on the given question.



Question: What is a crucial next step before applying the cleaning product to the glass?
 Reference: Pre-rinse the entire glass with cold water.
 Non-streaming: Wetting the surface with cold water.
 PEMF: Spray the cleaning solution onto the glass door and then use a scraper to gently lift the top layer of the hard water stains.
 video-SALMONN S: Wetting the glass with cold water.

Figure 11. Case study on non-streaming model, PEMF and video-SALMONN S in response to questions from ELViM. In this example, the woman has been holding the spray and a scraper in recent frames, and PEMF hallucinates that the woman is going to spray and scrape.



Question: What is inside the main white part?
 Reference: A small metal mesh filter
 Non-streaming: a ceramic disc and a red plastic component
 PEMF: A small metal pin in the center
 video-SALMONN S: A mesh filter

Figure 12. Case study on non-streaming model, PEMF and video-SALMONN S in response to questions from ELViM. In this video, both PEMF and non-streaming baseline fail to accurately identify the *mesh* structure of the internal.

D. FLOP Statistics

FLOP statistics are provided in Table 7. Incorporation of the TTT_{MEM} layer only adds a negligible overhead to TFLOPs compared to the entire Transformer.

Table 7. TFLOPs for video-SALMONN S

Configuration	TFLOPS
Qwen3-VL 8B	3.15
video-SALMONN S (w/o reading)	3.15+0.000235

E. Ablation Studies on Deepstack Embeddings

We provide the results in Table 8 to justify our design choice that only incorporates the TTT_{MEM} layer at the Transformer input, and performs direct downsampling/discard to the deepstack tokens. Including TTT_{MEM} for each stream of deepstack embeddings will multiply the additional memory and runtime overhead by at least 4, and also significantly increase training memory consumption.

Table 8. Accuracies on long-video benchmarks with TTT_{MEM} applied to only Transformer inputs and TTT_{MEM} applied to all 4 layers with deepstack embeddings for Qwen3-VL

Model	VideoMME (Short/Medium/Long)	LVBench
Inputs Only	76.4 (82.7/75.2/71.3)	55.4
Inputs + Deepstack	76.1 (82.2/76.0/70.1)	54.7

F. Further Results with Larger Memory

We conduct analysis with much larger memory budgets as long as it fits within a single H800 with 80GB memory, and the results are summarized in Table 9.

Table 9. Performance when further increasing the number of memory tokens. 128k tokens is the upper limit on a single H800 GPU.

Setup	Video-MME	LVBench	VideoEval-Pro	ELViM
32k Mem w/o reading	77.1 (82.9/76.3/72.0)	57.7	59.2	47.1
32k Mem w/ reading	77.3 (82.5/77.2/72.1)	57.9	61.0	49.4
128k Mem w/o reading	77.4 (82.8/77.1/72.4)	59.6	62.0	53.2
128k Mem w/ reading	77.3 (82.7/77.1/72.1)	59.8	62.3	54.9

G. Ablation Studies on the Prediction Spans

We show the accuracy against different prediction span settings in Fig. 10. All spans achieved equal or better performance compared to TTT without prediction. However, a longer span produces much noisier information and becomes less effective, and spans within one TTT minibatch do not have a large influence as well. Therefore, we choose 2 as the best trade-off.

Table 10. Performance of TTT-video and TTT_{MEM} with different prediction spans, T, on Video-MME long partition and LVBench with 16k memory tokens.

Span	Number of Tokens Intervals	Video-MME long	LVBench
TTT-video	—	70.0	54.3
T=1	1024	70.6	54.5
T=2	2048	71.3	55.4
T=4	4096	70.9	55.1
T=16	16384	71.0	54.8
T=32	32768	70.9	55.0